

MICROSTRUCTURES AND MICROCHEMISTRY OF SERPENTINES

A. BARONNET ⁽¹⁾, O. GRAUBY ⁽¹⁾, M. ANDRÉANI ⁽²⁾ y B. DEVOUARD ⁽³⁾

⁽¹⁾ CRM CN and University Paul Cézanne (Aix-Marseille III), Marseilles, France. baronnet@crmcn.univ-mrs.fr

⁽²⁾ LGM, IGP and University of Paris VI, Paris, France. andreani@ipgp.jussieu.fr

⁽³⁾ LMV, University Blaise Pascal, Clermont-Ferrand, France. B.Devouard@opgc.univ-bpclermont.fr

Serpentines are clay-sized hydrous magnesium silicates formed mostly by interaction of hot sea water with the basement of the oceanic crust and/or the upper mantle of the Earth (Mevel, 2003).

Using electron microscope techniques like FEGSEM, ATEM, HRTEM imaging and selected area electron diffraction we report on already known varieties as well as on new microstructures that escape from classical optical microscopy and X-ray diffraction analysis. We emphasize on crystallographic, nanostructural and compositional aspects of an updated list of microstructures that involve flat, curved, polygonal as well as polyhedral layers of serpentine. Atomically-resolved images and their Fourier transform analysis are presented also in support of still-debated details of curved and/or combined flat/curved structures of serpentine. The modulated structure of antigorite will not be addressed below.

The most abundant variety of serpentine is *lizardite*, only built-up by flat 1:1 layers. It crystallizes mostly as a columnar texture forming the rims of meshes in serpentinite matrices (Fig. 1). Their is an isovolumic, non-topotactic, replacement of forsterite by lizardite through sharp boundaries (Fig. 2), with large exportation of serpentine material and iron towards the serpentinite veins nearby. Such veins seem to mostly accommodate for the macroscopic swelling of the



Figura 1: Mesh texture of lizardite around olivine relicts. Polarizing microscope image between crossed nicols. Bigger olivine grain = 0.3 mm.

rock during hydration. In shear zones lizardite may display polysynthetic twinning on its basal plane (Fig. 3). It involves quasi periodic reversal of the 1:1 structure polarity along c^* . Lizardite composition extends from the pure Mg end-member towards amesite. This microstructure develops under small fluid/ solid ratios.

Protoserpentine is the most poorly-crystallized serpentine material. It is an intimate mixture of flat and curved nano pieces of serpentine material (Fig. 4). It replaces first decaying orthopyroxene in open alteration systems. We consider protoserpentine as a low-T and/or shortly-surviving, intermediate state between a pristine Mg-rich silicate gel and the better-crystallized rolled microstructures described below. Protoserpentine composition is quite variable but very close to that of more evolved structures forming from it.

Normal chrysotile looks up as achiral, multi-walled nanotubes, either forming scrolls or perfect cylinders (Yada, 1967; Amelinckx *et al.*, 1996). The inner hole radius is never smaller than 2 nm, and the outer

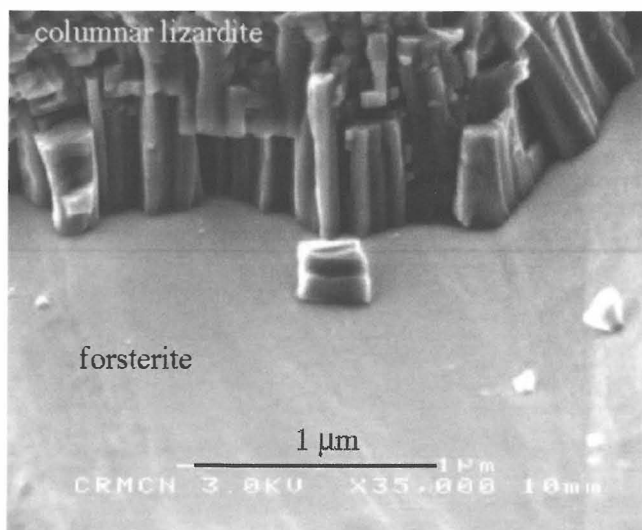


Figura 2: Intimate contact between columnar lizardite and a forsterite grain. 1:1 layers of serpentine are normal to the column axis. Columns run normal to the reacting substrate. Incipient voids between columns are probable pathways for water income to, and exportation of excess material from, the olivine/ lizardite interface. FEGSEM secondary electron image.

radius is always smaller than 50 nm (Fig. 5). Radial stacking is often semi-random. In veins, chrysotile forms various textures resembling those of frozen liquid crystals. Several cm-long chrysotile asbestos occurs in «crack-seal» veins where incremental growth takes place along vein selvages (Andréani et al., 2004). Chrysotile may evolve into 15-sectored or 30-sectored *polygonal serpentines* (Fig. 6) which are wider but shorter fibers. The structure of the flat lizardite-like sectors is sheared across sector boundaries where the 1:1 layer structure is curved

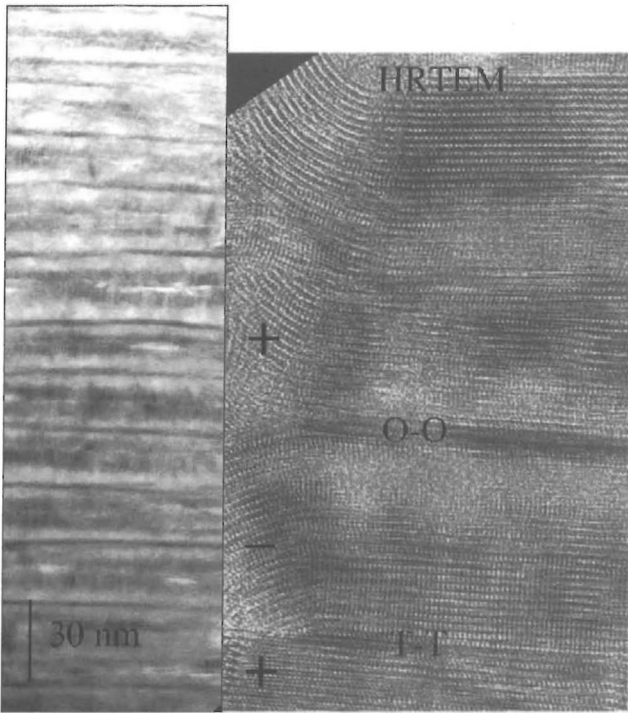


Figura 3: Polysynthetic twinning in sheared lizardite. Left: low-mag, bright-field TEM image showing quasi periodic sequences of twin doublets having reverse polarity (+ and -) of 1:1 layers in twin slabs. Right: <100> zone-axis HRTEM image of twin planes displaying octahedral-octahedral (O-O) contacts and tetrahedral-tetrahedral (T-T) contacts. These features are deduced from opposite curling of the layer blocks on prismatic faces of lizardite.

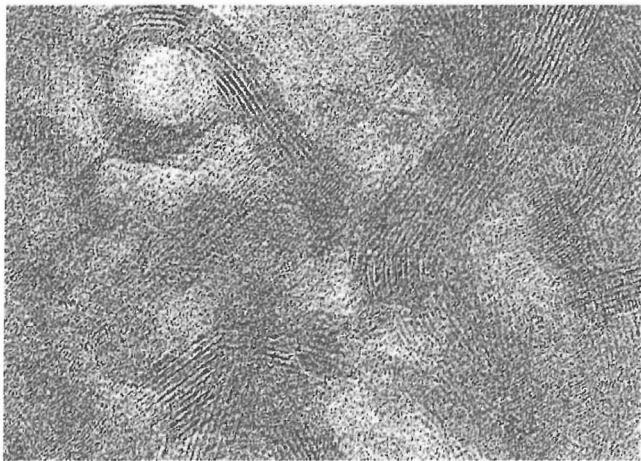


Figura 4: HRTEM, bright-field image of protoserpentine. Entangled nano tiles and plates form this poorly-crystallized serpentine material. 00l basal-lattice fringes are 0.72 nm apart.

around <100> and continuous (Baronnet & Devouard, 2005).

Synthetic *nano cones* are known for long in experimental charges (Yada & Iishi, 1974). We could find their natural equivalent in high-T serpentine veins which are coeval with olivine alteration (Fig. 7). These natural cones are always scrolled and thus imply periodic rotations of the serpentine lattice (Amelinckx et al., 1996). Their acute apex angles frequently satisfy optimal structure of the cone wall (Fig. 8) for which the conical lattice rotation reestablishes all H-bonds between successive turns.

The *polyhedral onions* (Baronnet et al., 2006) or *polyhedral serpentine grains* are a fascinating globular

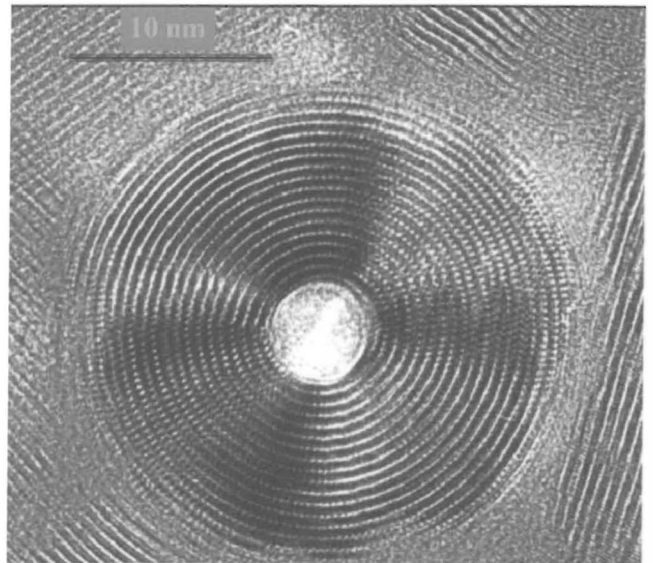


Figura 5: <100> zone-axis HRTEM image of the axial cross-section of a cylindrical chrysotile nano tube. Inner hollow tube 4 nm in diameter.

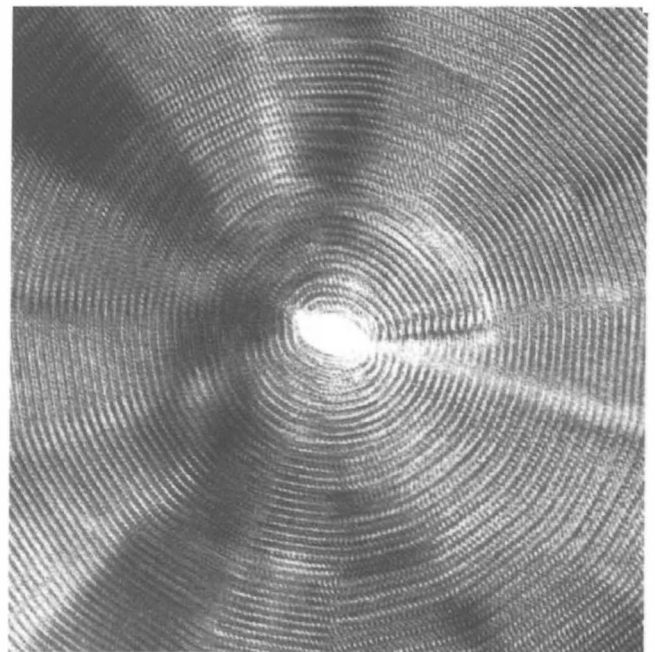


Figura 6: <100> zone-axis HRTEM image of the axial cross-section of the core of a polygonal serpentine fiber with fifteen sectors.

microstructure (Fig. 9) which might display more than 150 triangular facets when closed as a full sphere. The 1:1 layers are spherically wrapped and stacked to form a nested arrangement of pyramidal sectors. The tilt angle (14°) around $\langle 010 \rangle$ between neighbouring facets is controlled by all the 2-D possibilities to maintain all H-bonds between the layers. Selected area electron diffraction patterns indicate the conversion of more or

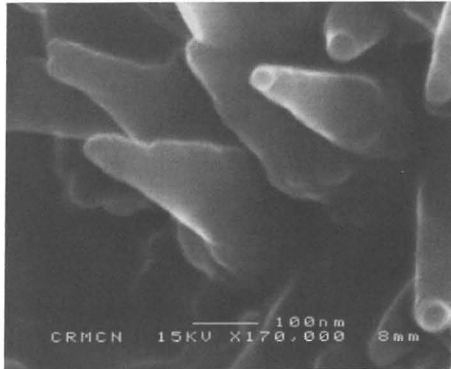


Figura 7: FEGSEM, secondary electron, image of serpentine nano cones protruding out from poorly-crystallized serpentine.

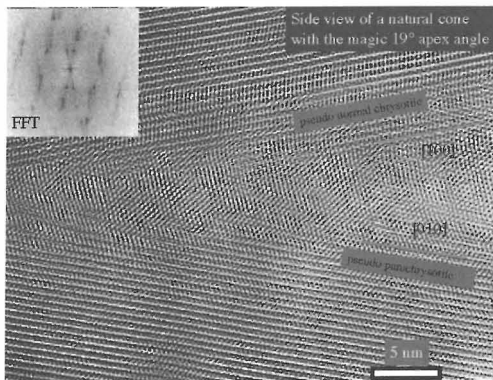


Figura 8: HRTEM image of a serpentine nano cone at atomic resolution. The apex angle is 19.6° , i.e., the one that allows recovery of the normal lizardite structure in the cone wall.

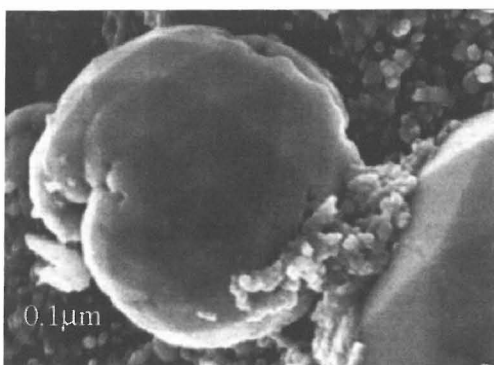


Figura 9: FEGSEM image of a grain of polyhedral serpentine showing a nice tiling of the sphere with triangular facets. No five-fold arrangement is visible. Grain diameter = $0.5 \mu\text{m}$.

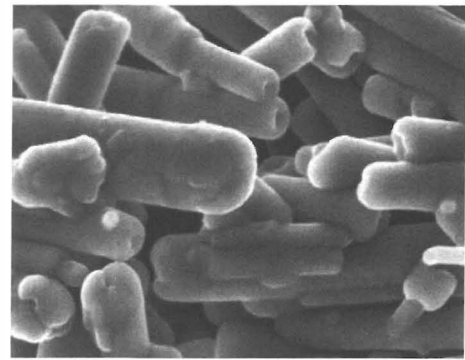


Figura 10: FEGSEM, low-voltage, secondary electron image of intergrown polygonal serpentine fibers with rounded closing caps. The biggest fiber is 200 nm in diameter. Note the «scepter of serpentine» made of an overgrown globular serpentine at the end of a short chrysotile nano tube in the lower-right corner of the image.

less disordered 1T into 1M polytypes and vice versa when crossing sector boundaries. Such onions nucleate as closing caps on chrysotile and polygonal serpentine (Fig. 10), and form from orthopyroxene alteration, most probably at lowest T during retrograde serpentinization. Such onions nucleate inside protoserpentine and acquire their euhedral habit in open cavities or cracks. The composition of polyhedral serpentine contains a significant amesite component.

From hydrothermal experiments in the MSH system at $P(\text{H}_2\text{O})$ below 1 kbar and $T = 250\text{-}450^\circ\text{C}$ (Grauby *et al.*, 1998), the above rolled structures could be ranked according to a decreasing order of metastability as protoserpentine, nanocones, chrysotile and polygonal serpentine, i.e., toward more and more crystallographic control of the layer stacking and of the curvature, and less and less curved parts in the microstructure. However, chrysotile shows a longer metastable persistence in the high-T range than at lower T where lizardite quickly forms. In the MASH system, introduction of Al (or Fe^{3+}) favors flat layers and shortens considerably the fibers. Experimental work to delineate the climate of formation of polyhedral serpentine is in progress.

REFERENCES

- Mevel, C. (2003). *C. R. Geoscience*, 335, 825-852.
 Yada; K. (1967). *Acta Crystallogr.*, 23, 704-707.
 Amelinckx, S., Devouard, B. y Baronnet, A. (1996). *Acta Crystallogr.*, A52, 850-878.
 Andréani, M., Baronnet, A., Boullier, A.-M., y Gratier, J.-P. (2004). *Europ. J. Mineral.*, 16, no 4, 585-596.
 Baronnet, A. & Devouard, B. (2005). *Canad. Mineral.*, 43, 513-542.
 Yada, K. y Iishi, K. (1974). *J. Crystal Growth* (1974), 24/25, 627-630.
 Baronnet, A., Andréani, M., Grauby, O., Devouard, B., Nitsche, S. y Chaudanson, D. (2006). *Amer. Mineral.* (2006), submitted.
 Grauby, O., Baronnet, A., Devouard, D., Schumaker, K. y Demirdjian, L. (1998). *Terra Nova*, suppl. 10(1), 24.